

Article

Synoptic and Climate Attributions of the December 2015 Extreme Flooding in Missouri, USA

Boniface Fosu ^{1,*}, Simon Wang ^{1,2}  and Kathleen Pegion ³

¹ Department of Plants, Soils and Climate, Utah State University, Logan, UT 84322, USA; simon.wang@usu.edu

² Utah Climate Center, Utah State University, Logan, UT 84322, USA

³ Department of Atmospheric, Oceanic, and Earth Sciences and Center for Ocean-Land-Atmosphere Studies, George Mason University, Fairfax, VA 22030, USA; kpegion@gmu.edu

* Correspondence: boniface.fosu@aggiemail.usu.edu; Tel.: +1-435-797-2233

Received: 21 January 2018; Accepted: 19 March 2018; Published: 21 March 2018



Abstract: Three days of extreme rainfall in late December 2015 in the middle of the Mississippi River led to severe flooding in Missouri. The meteorological context of this event was analyzed through synoptic diagnosis into the atmospheric circulation that contributed to the precipitation event's severity. The midlatitude synoptic waves that induced the extreme precipitation and ensuing flooding were traced to the Madden Julian Oscillation (MJO), which amplified the trans-Pacific Rossby wave train likely associated with the strong El Niño of December 2015. Though the near-historical El Niño contributed to a quasi-stationary trough over the western U.S. that induced the high precipitation event, an interference between the MJO and El Niño teleconnections resulted in a relatively weak atmospheric signature of the El Niño in comparison to that of the MJO. The influence of anthropogenic climate change on the relationship between ENSO and precipitation across several central U.S. states was also investigated using 17 CMIP5 models from the historical single-forcing experiments. A regime change in ENSO-related precipitation anomalies appears to have occurred, from being negatively correlated before 1950 to positive and significantly correlated after 1970, suggesting a likely effect of anthropogenic warming on the December 2015 extreme precipitation event.

Keywords: MJO; ENSO; flooding; greenhouse gases

1. Introduction

During late December 2015, a low-pressure system moved ashore onto the West Coast of the United States and later tracked northeastwards. This trough system induced a strong band of thunderstorms across the U.S. Central and Southern Plains, bringing unseasonably numerous tornadoes and unprecedented flooding (Figure 1a). The storm and its aftermath caused 50 fatalities and an estimated \$3 billion in damages in 13 U.S. states, with Missouri being the most impacted by flooding [1]. Several antecedent factors contributed to the severity of the flooding in Missouri: First, soil moisture conditions were saturated (Figure 1b) due to a consistently wet year with record rainfall in November (Figure 1c). Statewide precipitation was 300% of normal, making it the second-wettest December on record and the wettest since 1982 (Figure 1d). The soil conditions exacerbated the effect of the widespread rains received in December (not shown), before the late-December storm dropped about eight inches of precipitation. The atypical nature of the flooding is further highlighted by the time of year it occurred, since major precipitation and flooding events along the Mississippi River and Missouri have historically taken place in spring or summer (e.g., [2]).

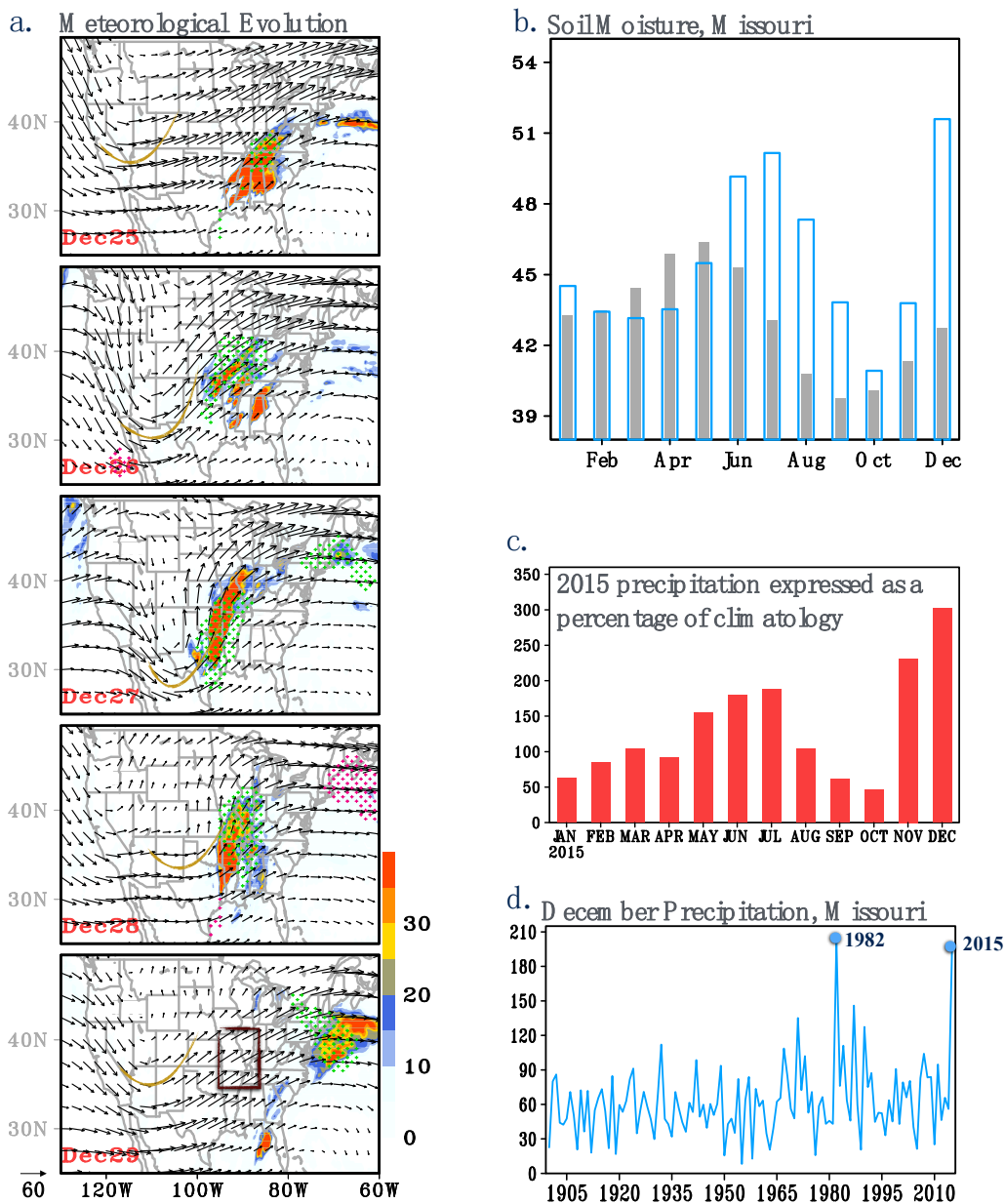


Figure 1. (a) Meteorological evolution of the late December event: 250-hPa winds (vectors) and precipitation (mm, shading), from 25–29 December 2015. Areas of positive (negative) vertically integrated (from 1000–300 mb) moisture flux convergence greater than $3 \times 10^{-4} \text{ kg s}^{-1}$ are represented by magenta (green) stippling. Upper-level short wave troughs are marked with yellow curves. The dark red box delineates the most affected storm areas, i.e., the study region; (b) 2015 monthly soil moisture (blue outline) (cm) in comparison to the 1950–2010 climatology (gray bars); (c) Monthly precipitation in 2015 expressed as a percentage of climatology. Each bar is representative of the total precipitation in each month of 2015 expressed as a percentage of that month’s climatology; (d) Interannual variation of statewide monthly precipitation in December for Missouri.

The persistent synoptic patterns associated with the flooding (Figure 1a) seem to suggest a modulation effect from large-scale circulation anomalies. During December 2015, the El Niño Southern Oscillation (ENSO) was at a near record positive phase, and it is well known that ENSO and its teleconnection can modulate the frequency of wintertime extremes in the U.S. (e.g., [3,4]). Coincidentally, a mature Madden Julian Oscillation (MJO) episode developed in December and appears to have interfered with the El Niño effect (Figure S1a). As the primary source of intraseasonal variability

in the Earth's climate system [5], the MJO's modulation of tropical convection can initiate poleward propagating Rossby waves that impact extratropical weather patterns and, in turn, influence the leading modes of low-frequency northern hemisphere variability, particularly in the Boreal winter [6,7].

Against this backdrop, the purpose of this study is to evaluate the extent to which large-scale circulation patterns associated with the El Niño and MJO may have facilitated the late-December 2015 extreme precipitation in Missouri. What's more, recent studies have reported that the ENSO teleconnection has enhanced under a warming climate, along with its impacts on the southern and central U.S. [8–10]. In view of this, we also investigate changes in ENSO-related precipitation across the central U.S. (with emphasis on West-North Central and the Southern Plains), particularly when forced by greenhouse gases and deduce the contribution of such changes to the severity of the 2015 Missouri flooding.

The rest of the paper is structured as follows: in Section 2, we outline the methods used to align the typical MJO phase with this case in December 2015, as well as the approach used for assessing the role of the El Niño teleconnection. We move on to results and discussions in Section 3, and provide some concluding remarks in Section 4.

2. Data and Methodology

2.1. Data Sources

The Climate Prediction Center's (CPC) model-calculated monthly soil moisture at 0.5° grid spacing is used to estimate monthly soil moisture anomalies [11]. For precipitation, we utilize the CPC morphing technique [12] and the Parameter-Elevation Regressions on Independent Slopes Model [13] datasets for daily and monthly fields, respectively. To analyze atmospheric circulation, output from the National Centers for Environmental Prediction/National Center for Atmospheric Research (NCEP/NCAR) global reanalysis at 2.5-degree resolution is used [14].

Attribution analysis is carried out by assessing long-term changes to ENSO's teleconnection impact on precipitation across the central U.S. using 17 models from phase 5 of the Coupled Model Intercomparison Project (CMIP5). We specifically analyze two historical single-forcing experiments, i.e., the natural-only forcing (NAT) and the greenhouse gas (GHG)-only forcing [15]. Each experiment produced multiple members initialized from a long-stable preindustrial (1850) control run up to 2005. Table S1 in the supporting information provides the full name, institute, ensemble size, and spatial resolution of each model.

2.2. Determining Relevant MJO Phases

The MJO has often been identified by use of an empirical orthogonal function (EOF) analysis. In this study, the state of the MJO is defined by projecting daily anomaly data onto the leading pair of empirical orthogonal functions (EOFs) of equatorially averaged (15° S–15° N) 200 hPa velocity potential (χ_{200}) fields. The EOF analysis covers a three-month period (1 December–28 February), and is performed on a yearly basis between 1979 and 2015. Prior to the EOF computation, χ_{200} is bandpass filtered to the intraseasonal period of 30–60 days to isolate the MJO signal, a method dating back to several MJO studies. The MJO can also be viewed in a two-dimensional phase space defined by the two-leading pair of principal component (PC) from the EOF analysis. Since the phase space diagram is a method for observing both the amplitude and the phase of the MJO during its propagation, we construct yearly phase space diagrams and use them to identify "MJO activity days", defined as days when the MJO amplitude (i.e., $\sqrt{PC1^2 + PC2^2}$) is greater than or equal to one [16]. Note that before the phase space diagrams are constructed, the two PCs are normalized with their respective mean and standard deviation [17].

This approach generally follows the methodology of [18] but unlike WHO4, we use velocity potential (χ_{200}) for the EOF representation instead of a combination of OLR, 850-hPa zonal wind (u850) and 200-hPa zonal wind (u200). Reference [19] shows that OLR is a relatively noisy field both spatially

and temporally, with variability mostly limited to the Eastern Hemisphere. Additionally, the inverse Laplacian used to calculate χ_{200} acts as a smoother, which makes χ_{200} more sensitive to global-scale variations of divergence rather than being concentrated on the Indo-Pacific warm pool like OLR.

2.3. Synoptic Attribution Methods

This section outlines the attribution methods employed to assess the relative contributions of the MJO and El Niño to the synoptic conditions associated with the late December 2015 extreme rainfall, and subsequent flooding in Missouri. This is quite a lengthy section, but is necessary to properly interpret the ensuing results from our diagnostic methods.

2.3.1. The 2015 December MJO Episode

First, the spatial representation and evolution of the MJO event during which the late-December 2015 Missouri flooding occurred is constructed. For the remainder of this paper, we call this MJO event the “December MJO episode”. In accordance with the phase space diagram for the year 2015, the spatial evolution of the December MJO episode is developed by averaging all MJO activity days (i.e., amplitude ≥ 1) in each given phase. This is done for both 200 hPa velocity potential (χ_{200}) and streamfunction (ψ_{200}) over a domain spanning the globe longitudinally and from latitude 40° S–80° N. Both χ_{200} and ψ_{200} are bandpass-filtered within a 30–60 days intraseasonal frequency.

Next, we take an approach based on the idea that the contribution of the December MJO episode to the synoptic conditions that caused the Missouri flooding can be statistically separated. This can be achieved through regression analysis that involves an “MJO phase composite” comprising past MJO events with identical characteristics to the December 2015 MJO episode. In line with this, 36 MJO episodes before 2015 are constructed on a yearly basis, from 1979 to 2014, by following the initial steps outlined above. The so-called MJO phase composite is created from these 36 MJO episodes. However, before the composition is done, we take measures to ensure that the eight phases of the MJO phase composite can correctly align with the corresponding phases of the December 2015 MJO episode. This is necessary for two reasons: First, it provides an objective basis for a more direct empirical comparison between the MJO’s general structure and the December episode. Second, it ensures that the MJO phase composite can serve to attribute the source of the December 2015 circulation anomalies.

To achieve the aforementioned alignment, corresponding phases of the December 2015 MJO episode and past MJO episodes are subjected to a spatial correlation analysis. If the resulting correlation coefficients at all eight phases for any past episode remains robust above 0.8, that episode is retained. Twenty five out of the 36 past MJO episodes satisfy the criteria and are synthesized to create two MJO phase composites—one for χ_{200} and the other for ψ_{200} .

2.3.2. MJO Related Anomalies

The MJO’s contribution to the synoptic conditions that led to the late-December 2015 Missouri flooding is calculated by linearly regressing the eight phases of the 2015 December MJO episode on the eight phases of the MJO phase composite. This can be expressed by

$$Y_{(x,y)} = \alpha X_{(x,y)} + b$$

where Y and X are the December MJO episode and the MJO phase composite, respectively, and both are on a spatial longitude-latitude (lat-lon) domain. The regression coefficient α is considered an estimate of the historical effect of the MJO in December. Therefore $\alpha_{(x,y)}$ is composed of the regression coefficients of several time series regressions at every given grid point within a specified domain. Consider a least-squares regression between two datasets with eight time steps (representative of the MJO phases) over a lat-lon domain (i.e., 180° E–180° W, 40° S–80° N), instead of a regression between two sets of time series. At this point, the statistical estimation of the MJO “component” of the

December 2015 circulation anomalies becomes possible by multiplying the regression output $\alpha_{(x,y)}$ to the December MJO episode at every phase. This is done for both χ_{200} and ψ_{200} .

One may argue that a more straightforward calculation of the MJO's contribution to the flooding could be achieved by simply replacing the MJO phase composite with MJO amplitude in the regression. However, MJO amplitude is calculated from the two leading principal components (PCs) generated through EOF analysis (i.e., $amplitude = \sqrt{PC1^2 + PC2^2}$) and, therefore, will not include the phase information of the MJO in a regression. While the WH04 RMM indices or PC's of MJO proxies have emerged as the optimal way of explaining MJO variability, unless taken together, a single PC index by itself cannot explain all the variability associated with the MJO. On the other hand, employing the phase composite as used here accounts for both the amplitude of the MJO and its "correct" phase, which is critical in terms of the actual MJO event days. Although somewhat unconventional, our composite approach ensures that both the phasing and amplitude of the MJO are accounted for in the regression.

2.3.3. ENSO-Related Anomalies

On the seasonal timescale, the effect of the strong El Niño in December 2015 on circulation is also assessed. The ENSO signal is defined as the Niño 3.4 index (N34), i.e., the normalized SST anomaly over the 5° S–5° N and 170° W–120° W region of the Pacific Ocean. Here, we use monthly N34 anomalies to approximate the impact of ENSO during each phase of the MJO. For each MJO phase, monthly N34 values are assigned to the 25 previously selected past MJO episodes. The initial outcome is a 25-point index for each MJO phase. However, for the subsequent regression analysis, we only use a version of each index with N34 anomalies greater than one standard deviation (i.e., strong ENSO events), which we call a "strong N34 index". While this may appear subjective, it follows previous research that during weak ENSO events, there is no clear Pacific/North American oscillation pattern that prevents influential energy propagation towards the continental U.S. [20,21].

To calculate the portion of circulation anomalies attributable to ENSO, ψ_{200} (on a spatial domain) is regressed on the strong N34 index at every phase. The resulting regression outputs are taken as representative of the historic ENSO effect on each MJO phase. We then multiply the regression outputs by values of the N34 index corresponding to the 2015 December MJO episode, to obtain statistical estimates of the December 2015 circulation anomalies attributable to the El Niño by phase.

Once the attributable components of the MJO and ENSO have been calculated for the December MJO episode, a synoptic attribution analysis is carried out. For χ_{200} , we only remove the MJO component (i.e., the portion of the circulation anomalies attributable to the MJO) from the December MJO episode. For ψ_{200} , both the MJO and ENSO components (i.e., the typical MJO impact, plus strong ENSO signals regressed out of the 2015 December MJO signal) are removed. What is left, the residual, is then regarded as the portion of the circulation that cannot be explained by ENSO and the MJO.

3. Results and Discussion

Figure 1 shows the synoptic evolution leading up to the late-December 2015 extreme precipitation event and the characteristics of the moisture fields associated with it. Precipitation occurred during an extended period (25–28 December 2015) over several central U.S. states in a band of thunderstorms generally stretching from Illinois to Texas, with a center over Missouri. Concomitant with this was a quasi-stationary trough over the western U.S., which deepened prior to inducing the strongest precipitation event on December 27. The anomalies of vertically integrated moisture flux as shown in Figure 1 are markedly effective in highlighting the strongest areas of moisture transport associated with the heaviest rainfall, where instability remained strong upstream of the trough along the axis of the mean wind.

To characterize the December 2015 circulation patterns and associated ENSO teleconnection, we first show in Figure 2a a regression of the Niño 3.4 index on 250-hPa height anomalies from 1950 to 2014, in comparison with the December 2015 circulation anomalies plotted in Figure 2b. A trans-pacific wave train emanating from Asia into North America is discernable in both cases and depicts an

anomalous Aleutian low over the Northern Pacific with a height anomaly of opposite polarity over the Plains states (e.g., [22]).

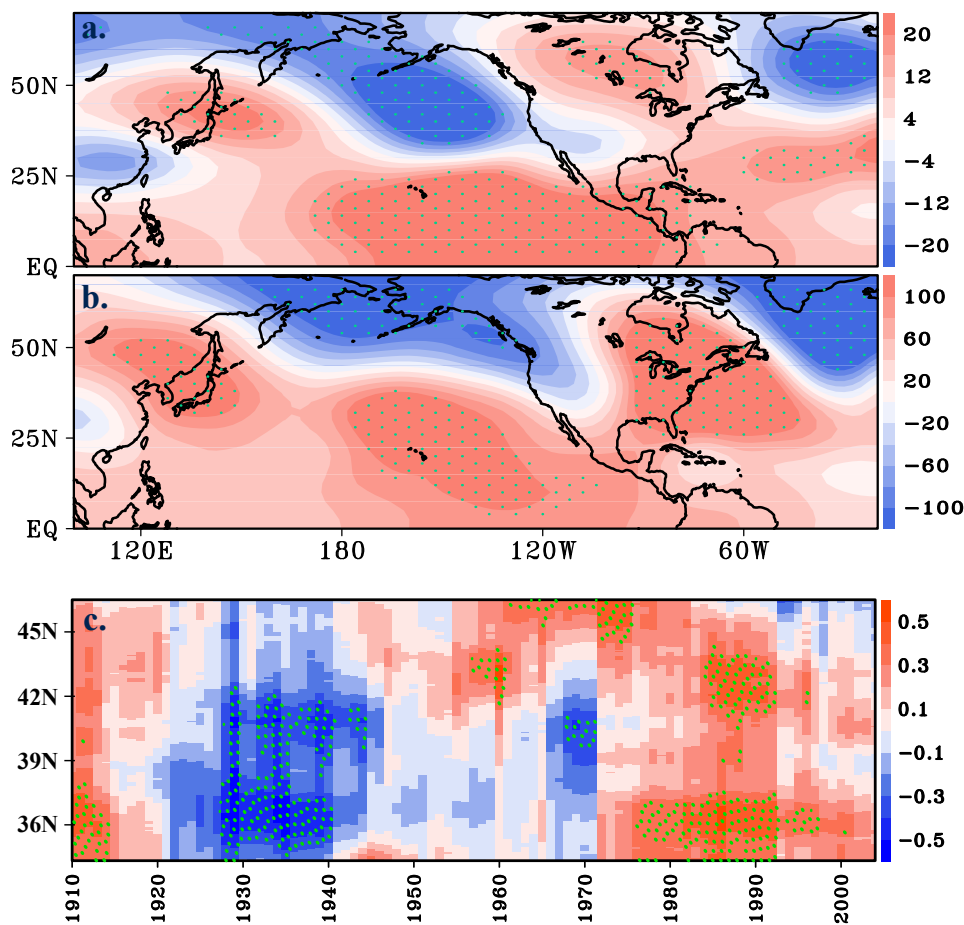


Figure 2. (a) Regression of 250-hPa height anomalies with Niño 3.4 in December, from 1950–2014; (b) December 2015 250 hPa height anomalies as a departure from the 1950–2010 base period; (c) Latitude-time plot of the 20-years sliding correlation between Niño 3.4 and December precipitation averaged over longitude 95° W–85° W. On the x-axis are the central years of the correlation window. Green stippling show significant areas at the 95% confidence level.

Next, we illustrate in Figure 2c the Hovmöller diagram of the 20-year sliding correlation between Niño 3.4 and precipitation averages along a longitudinal cross-section of the central U.S. (95° W–85° W; during December), to depict the link between the changing ENSO teleconnection pattern and local precipitation response. The 20-year sliding window is chosen to examine the decadal-scale variations between ENSO and precipitation [23]. There is an apparent “regime change” in the ENSO-related precipitation anomalies across the target region, from being negatively correlated before 1950 to positively and significantly correlated after 1970. This implies a general amplification effect of the El Niño teleconnection on Southern Plains precipitation, as was reported in [10,24]. Different sliding windows ranging from 10 to 25 years were also tested. The result (not shown) does not indicate any significant difference in the correlation pattern.

The MJO episodes embedded in the December 2015 event are also examined. Figure 3a illustrates the evolution of the global χ_{200} from early December to mid-January, revealing an eastward-propagating pattern that shows a clear association with the MJO. As expected, the December MJO episode (Figure 3a) and the corresponding composite of past MJO cycles (Figure 3b; created from the alignment method introduced in Section 2.3.1) show a coherent eastward propagation.

While it may be difficult to differentiate between the two patterns, the residual plot in Figure 3c, computed by subtracting Figure 3b from Figure 3a, shows only regional and somewhat stationary features. This implies that the MJO did have a discernable impact on the global divergent circulation during December 2015. The inadvertent difference in magnitude between the phases of the December MJO episode and that of the composite may be considered a limitation in our regression approach. Although all MJO event days are selected using the same criteria, the magnitude of a well-defined MJO event (amplitude ≥ 1 for consecutive pentads and lasts longer than 25 days, Figure S1b) like the December episode would always be greater than that of any MJO composite. However, the correct phase of the MJO is equally as important as its amplitude to North American weather [7,25,26] and is a key factor in the context of this study.

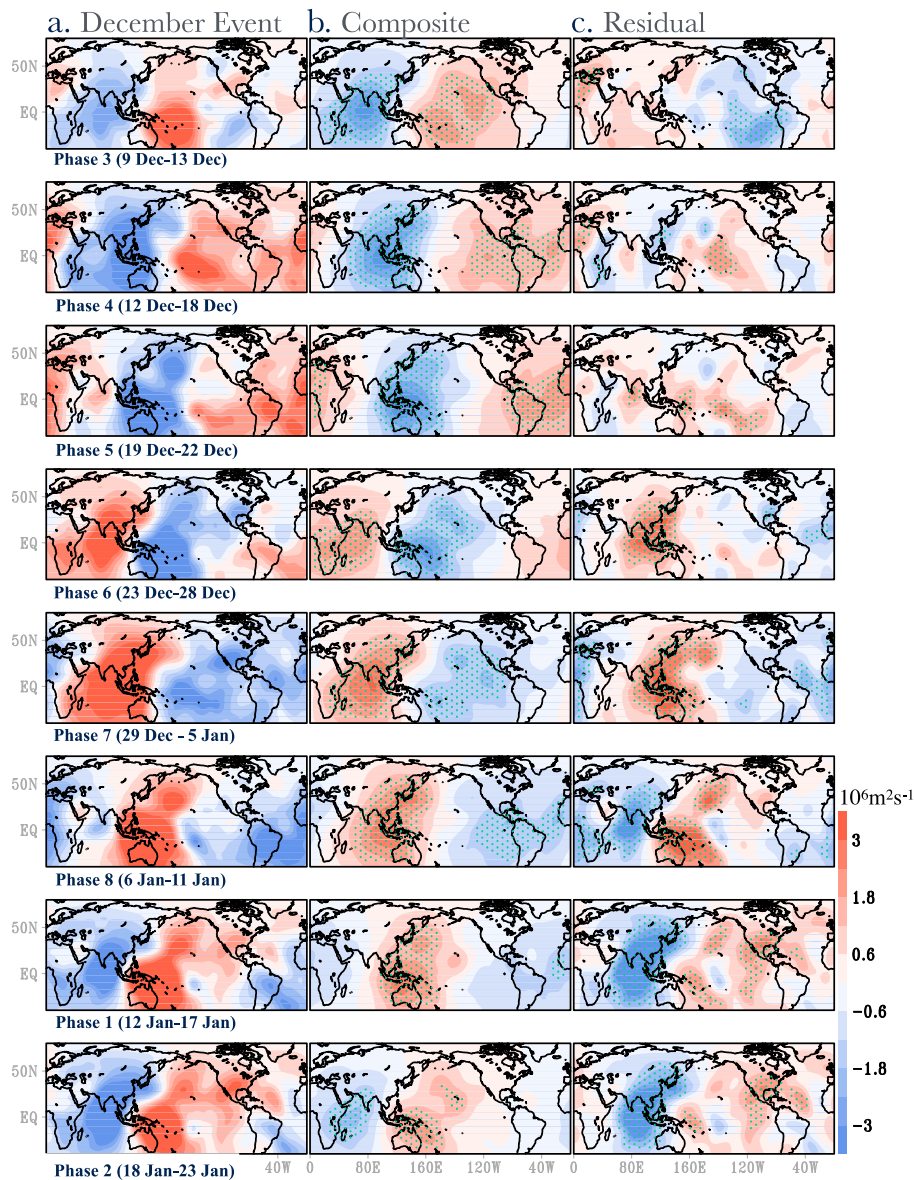


Figure 3. (a) 200-hPa velocity potential anomalies based on the eight phases of the December 2015 MJO episode described in the text; (b) Composite of 200-hPa velocity potential anomalies based on 25 prior MJO episodes; (c) Velocity potential anomalies not linearly explained by the MJO (i.e., linearly regressed construction of the MJO’s impact subtracted from the December event anomalies of χ). Green stippling show significant areas at the 95% confidence level.

One of the fundamental and underlying mechanisms by which tropical convection, such as that associated with the MJO, excites Pacific/North American (PNA) like teleconnection patterns (see Figure 2a) is through the linear dispersion of a Rossby wave triggered by tropical heating [25]. To examine this extratropical wave train induced by the MJO's convective forcing, we repeat the analyses of Figure 3 using ψ_{200} . This time, we superimpose the wave-activity flux for stationary waves, as derived by Takaya and Nakamura 2001 (Figure 4). The general characteristics of the anomalous circulation patterns between the December 2015 MJO cycle (Figure 4a) and the composite MJO cycle (Figure 4b) are similar. Focusing on the period prior to the floods (Phase 6), strong Rossby wave trains steadily propagate eastward from the tropical Pacific towards North America during the preceding weeks (phases 4 and 5; Figure 4a). The circulation patterns from phases 4 to 6, particularly in phase 6, resemble the ENSO-induced teleconnection pattern; these are consistent with previous findings that MJO-storm track variability associated with ENSO and phases 5 and 6 of MJO have qualitatively similar characteristics to that associated with the PNA [27,28]. Furthermore, Figure 4a lends support to the notion that it takes a week for any tropical diabatic heating signal to propagate into North America [29] and about 2 weeks for the extratropical response to fully develop [30]. The relatively strong amplitude of the December MJO (see Figure S1b) forced the eastward flux of Rossby waves which, in turn, triggered robust extratropical atmospheric responses prior to phase 6 (the storm event), as shown by streamfunction and the wave activity flux in Figure 4.

The residuals in Figure 4c reflect what is left from the December 2015 cycle after the linear removal of the combined impacts of the MJO and ENSO, as outlined in Sections 2.3.2 and 2.3.3. Of the remaining circulation anomalies, the wave-activity flux in Figure 4c does not resemble any prominent teleconnection source, and therefore mostly comes from internal variability associated with synoptic disturbances over the north Pacific. It is important to mention that only the removal of strong ENSO events as discussed earlier had a noteworthy impact on the anomalous circulations as seen in Figure 4c. Yet, ENSO's effect was not as large as the MJO's subseasonal contribution. These results demonstrate that the synoptic patterns associated with the heavy precipitation can be primarily attributed to MJO-related circulation anomalies.

As is shown in [31,32], the extratropical response to the MJO is enhanced when MJO-related convection is in phase with heating and convection anomalies associated with certain ENSO phases. However, attempts to uncover a systematic relationship between the MJO and ENSO have yielded conflicting results [33] due to nonlinearity in their combined impact [32]. Reference [6] showed that the occurrence probabilities of Pacific North America (PNA) like MJO teleconnection patterns are more likely to occur during El Niño periods than during La Niña or neutral periods, while a more recent study by [34] shows that strong MJO activity significantly weakens the atmospheric branch of ENSO. That said, the simple fact that ENSO imprints are longer than the episodic MJO phases makes attribution difficult. These are the likely reasons why the atmospheric signature of a near historical El Niño was relatively weak in comparison to the MJO during late December 2015.

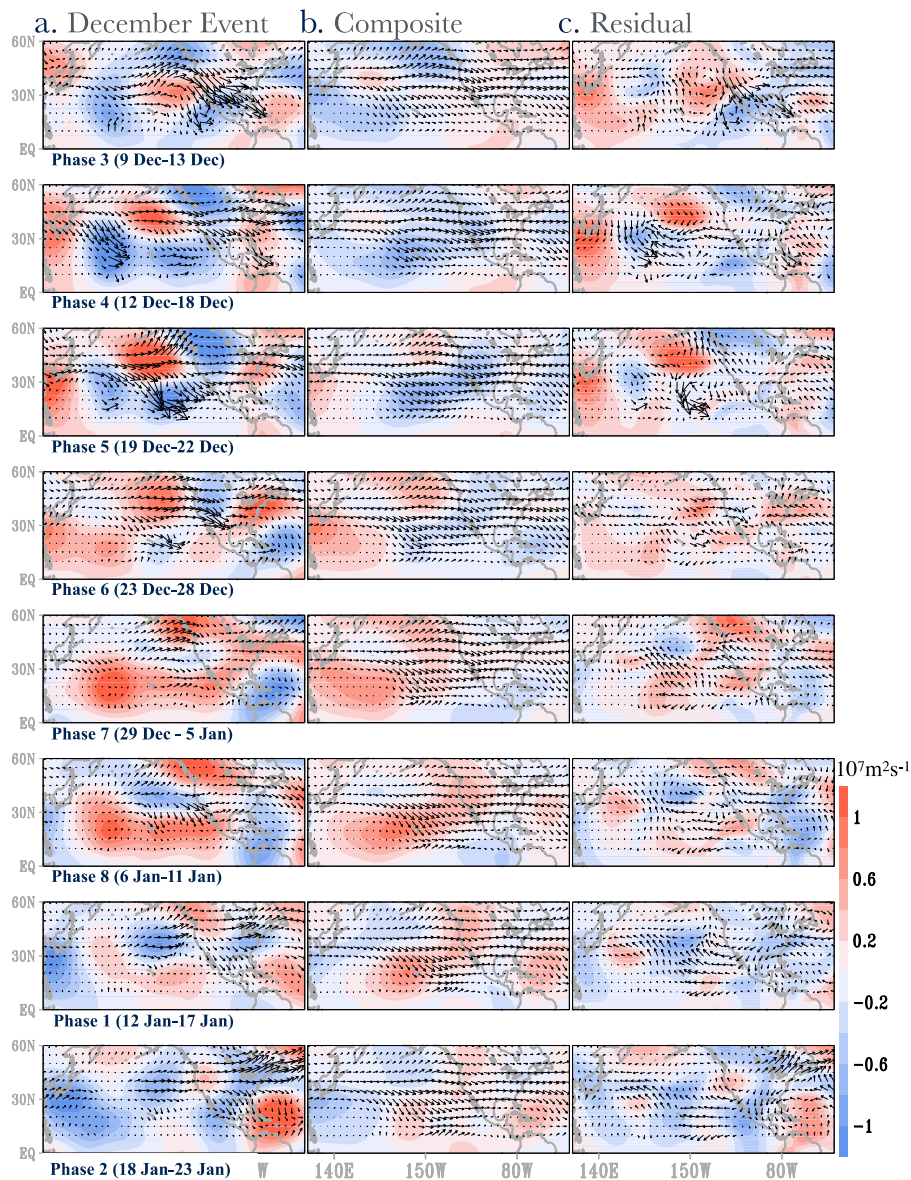


Figure 4. (a) 200-hPa streamfunction anomalies based on the eight phases of the December 2015 MJO episode described in the text; (b) Composite of 200-hPa streamfunction anomalies based on 25 prior MJO episodes; (c) Streamfunction anomalies not linearly explained by the MJO and ENSO (i.e., linearly regressed constructed impact of both the MJO and ENSO subtracted from the December event anomalies of Ψ). Corresponding wave-activity fluxes are superimposed in vectors.

Climate Change Impacts

Recall that Figure 2c depicts a regime change in the ENSO-related precipitation anomalies across several parts of the Central and Southern Plains. To attribute the causes of this apparent regime change, we repeat the analysis in Figure 2c using two forcing scenarios of 17 CMIP5 models. The result is presented in Figure 5—the CMIP5 representation of the 20-year sliding correlation between the Nino-3.4 index and precipitation. In the GHG run (Figure 5a), the model spread (contours), along with the ensemble mean (shading), which is the composite mean of 17 models (Table S1), depict a general strengthening of the relationship between ENSO and precipitation across the central U.S. Note that only statistically significant contours at the 95% confidence level are drawn. On the contrary, the NAT run (Figure 5b) exhibits a relatively weak relationship between ENSO and precipitation. Although this result does not directly address the impact of climate change specifically on the December 2015 Missouri

flooding, it does lend support to the observations (Figure 5c) and previous studies [10] that the regime change in the ENSO-induced precipitation anomalies across the Southern Plains is likely linked to the warming climate. Further examination of the MJO's effect on precipitation in the Southern Plains will be needed when the CMIP5 models' performance in the tropical intraseasonal variability is improved.

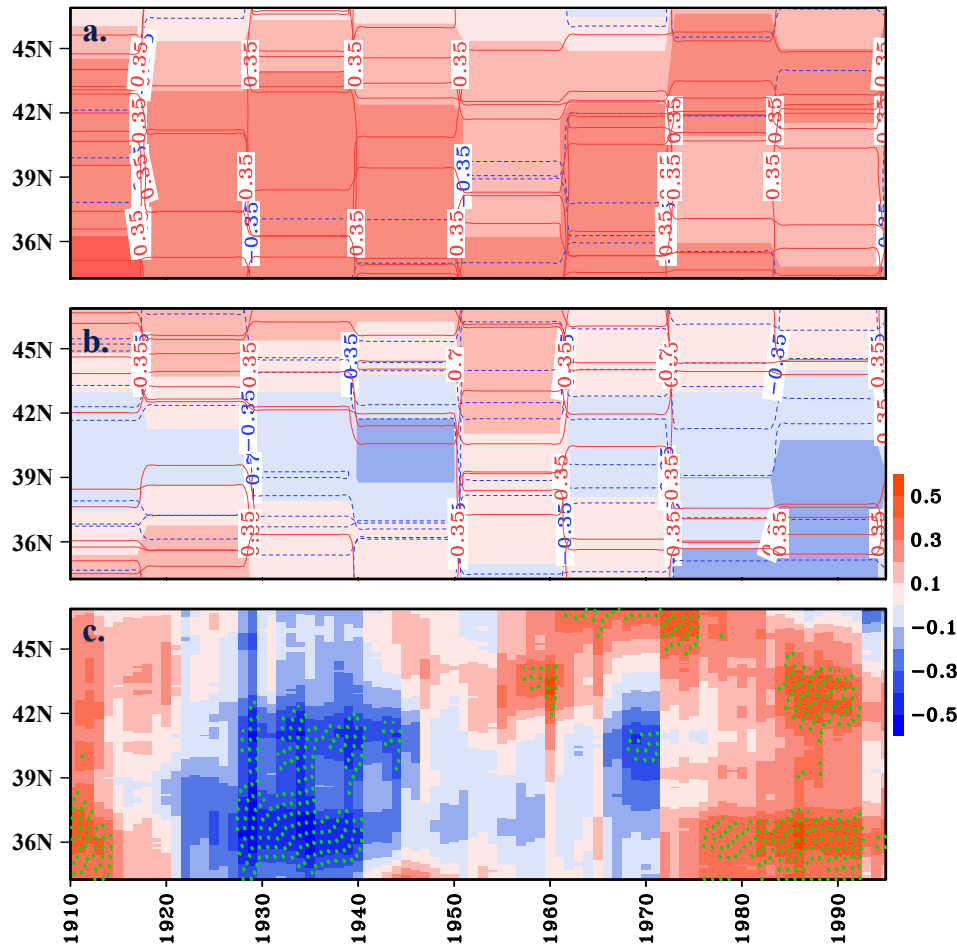


Figure 5. 20-years sliding correlation between the December Nino 3.4 index and precipitation averaged longitudinally over 95° W– 85° W, as depicted by 17 CMIP5 models in two scenarios—(a) GHG run and (b) Natural run. Shading represents the ensemble mean. Years on the x axis represent the central years of the sliding window. The ensemble spread is in contours and only statistically significant contours at the 90% confidence level are drawn. Figure 5c is a repeat of Figure 2c with a comparable timespan to the model runs.

4. Concluding Remarks

The spatial and temporal features of the large-scale circulation anomalies associated with the late-December 2015 flood in Missouri were analyzed. Through synoptic attribution analyses, we found an interference between certain MJO phases and the El Niño during the time leading up to the Missouri flood. Consequently, an unusually high precipitation event occurred during phase 6 of the MJO cycle, i.e., from 23 to 28 December 2015. At this time, the MJO's convection amplified a trans-Pacific Rossby wave train that resembles the ENSO-driven teleconnection pattern from the tropics to form the interference. This contributed to an energized upper-level circulation and strong jet stream flow over the contiguous United States and led to the advection of intense cyclone activity into the Central and Southern Plains [35]. In the long term, the effect of anthropogenic warming on the December event is also implied through the analysis of several CMIP5 models. The models suggest that the response of precipitation in the central U.S. to ENSO would be enhanced owing to a warming

climate. With this study, we seek to provide a meaningful contribution to the literature on the synoptic attribution of climate extremes.

Supplementary Materials: The following are available online at <http://www.mdpi.com/2073-4441/10/4/350/s1>, Figure S1: Additional information on the December 2015 MJO episode, Table S1: Full name, institute, ensemble size, and spatial resolution of the CMIP5 models used.

Acknowledgments: This study was supported by the SERDP grant RC-2709 and the Utah Agricultural Experiment Station, Utah State University, and approved as journal paper number 9085.

Author Contributions: B.F. and S.W. designed the research and wrote the main part of the manuscript. B.F., S.Y. and K.P. contributed to the writing of the paper, analyses and discussion of results and review of the manuscript.

Conflicts of Interest: The authors declare no conflict of interest.

References

- Holmes, R.R.; Watson, K.M.; Harris, T.E. *Preliminary Peak Stage and Streamflow Data at Selected U.S. Geological Survey Streamgages for Flooding in the Central and Southeastern United States during December 2015 and January 2016: U.S. Geological Survey Open-File Report 2016–1092*; U.S. Geological Survey: Reston, VA, USA, 2016; p. 27.
- Hirschboeck, K.K. Climates and floods. In *National Water Summary 1988-89 Floods and Droughts: Hydrologic Perspectives on Water Issues*; Paulson, R.W., Chase, E.B., Roberts, R.S., Moody, D.W., Eds.; U.S. Geological Survey: Reston, VA, USA, 1991; pp. 67–88. Available online: <http://pubs.usgs.gov/wsp/2375/report.pdf> (accessed on 12 June 2016).
- Higgins, R.W.; Schemm, J.K.E.; Shi, W.; Leetmaa, A. Extreme precipitation events in the Western United States related to tropical forcing. *J. Clim.* **2000**, *13*, 793–820. [[CrossRef](#)]
- Schubert, S.D.; Chang, Y.; Suarez, M.J.; Pegion, P.J. ENSO and wintertime extreme precipitation events over the contiguous United States. *J. Clim.* **2008**, *21*, 22–39. [[CrossRef](#)]
- Zhang, C. Madden-Julian oscillation: Bridging weather and climate. *Bull. Am. Meteorol. Soc.* **2013**, *94*, 1849–1870. [[CrossRef](#)]
- Riddle, E.E.; Stoner, M.B.; Johnson, N.C.; L’Heureux, M.L.; Collins, D.C.; Feldstein, S.B. The impact of the MJO on clusters of wintertime circulation anomalies over the North American region. *Clim. Dyn.* **2013**, *40*, 1749–1766. [[CrossRef](#)]
- Rodney, M.; Lin, H.; Derome, J. Subseasonal Prediction of Wintertime North American Surface Air Temperature during Strong MJO Events. *Mon. Weather Rev.* **2013**, *141*, 2897–2909. [[CrossRef](#)]
- Meehl, G.A.; Tebaldi, C.; Teng, H.; Peterson, T.C. Current and future U.S. weather extremes and El Niño. *Geophys. Res. Lett.* **2007**, *34*, L20704. [[CrossRef](#)]
- Stevenson, S.; Fox-Kemper, B.; Jochum, M.; Neale, R.; Deser, C.; Meehl, G. Will There Be a Significant Change to El Niño in the Twenty-First Century? *J. Clim.* **2012**, *25*, 2129–2145. [[CrossRef](#)]
- Wang, S.-Y.; Huang, W.-R.; Hsu, H.-H.; Gillies, R.R. Role of the strengthened El Niño teleconnection in the May 2015 floods over the southern Great Plains. *Geophys. Res. Lett.* **2015**, *42*, 8140–8146. [[CrossRef](#)]
- Fan, Y.; van den Dool, H. Climate Prediction Center global monthly soil moisture data set at 0.5° resolution for 1948 to present. *J. Geophys. Res.* **2004**, *109*, D10. [[CrossRef](#)]
- Joyce, R.J.; Janowiak, J.E.; Arkin, P.A.; Xie, P. CMORPH: A method that produces global precipitation estimates from passive microwave and infrared data at high spatial and temporal resolution. *J. Hydrometeorol.* **2004**, *5*, 487–503. [[CrossRef](#)]
- Daly, C.; Halbleib, M.; Smith, J.I.; Gibson, W.P.; Doggett, M.K.; Taylor, G.H.; Curtis, J.; Pasteris, P.A. Physiographically-sensitive mapping of temperature and precipitation across the conterminous United States. *Int. J. Climatol.* **2008**, *28*, 2031–2064. [[CrossRef](#)]
- Kalnay, E.; Kanamitsu, M.; Kistler, R.; Collins, W.; Deaven, D.; Gandin, L.; Iredell, M.; Saha, S.; White, G.; Woollen, J.; et al. The NCEP/NCAR 40-year reanalysis project. *Bull. Am. Meteorol. Soc.* **1996**, *77*, 437–471. [[CrossRef](#)]
- Taylor, K.E.; Stouffer, R.J.; Meehl, G.A. An overview of CMIP5 and the experiment design. *Bull. Am. Meteorol. Soc.* **2012**, *93*, 485–498. [[CrossRef](#)]
- Zhou, S.; L’Heureux, M.; Weaver, S.; Kumar, A. A composite study of the MJO influence on the surface air temperature and precipitation over the Continental United States. *Clim. Dyn.* **2012**, *38*, 1459–1471. [[CrossRef](#)]

17. Kiladis, G.N.; Dias, J.; Straub, K.H.; Wheeler, M.C.; Tulich, S.N.; Kikuchi, K.; Weickmann, K.M.; Ventrice, M.J. A comparison of OLR and circulation-based indices for tracking the MJO. *Mon. Weather Rev.* **2014**, *142*, 1697–1715. [[CrossRef](#)]
18. Wheeler, M.C.; Hendon, H.H. An All-Season Real-Time Multivariate MJO Index: Development of an Index for Monitoring and Prediction. *Mon. Weather Rev.* **2004**, *132*, 1917–1932. [[CrossRef](#)]
19. Ventrice, M.J.; Wheeler, M.C.; Hendon, H.H.; Schreck, C.J.; Thorncroft, C.D.; Kiladis, G.N. A Modified Multivariate Madden–Julian Oscillation Index Using Velocity Potential. *Mon. Weather Rev.* **2013**, *141*, 4197–4210. [[CrossRef](#)]
20. Huang, J.; Higuchi, K.; Shabbar, A. The relationship between the North Atlantic Oscillation and El Niño–Southern Oscillation. *Geophys. Res. Lett.* **1998**, *25*, 2707–2710. [[CrossRef](#)]
21. Mourtzinis, S.; Ortiz, B.V.; Damiandis, D. Climate Change and ENSO Effects on Southeastern US Climate Patterns and Maize Yield. *Sci. Rep.* **2016**, *6*, 29777. [[CrossRef](#)] [[PubMed](#)]
22. Chen, T. A North Pacific Short-Wave Train during the Extreme Phases of ENSO. *J. Clim.* **2002**, *15*, 2359–2376. [[CrossRef](#)]
23. McCabe, G.J.; Dettinger, M.D. Decadal variations in the strength of ENSO teleconnections with precipitation in the western United States. *Int. J. Climatol.* **1999**, *19*, 1399–1410. [[CrossRef](#)]
24. Bonfils, C.J.; Santer, B.D.; Phillips, T.J.; Marvel, K.; Leung, L.R.; Doutriaux, C.; Capotondi, A. Capotondi Relative Contributions of Mean-State Shifts and ENSO-Driven Variability to Precipitation Changes in a Warming Climate. *J. Clim.* **2015**, *28*, 9997–10013. [[CrossRef](#)]
25. Johnson, R.H.; Ciesielski, P.E. Structure and Properties of Madden–Julian Oscillations Deduced from DYNAMO Sounding Arrays. *J. Atmos. Sci.* **2013**, *70*, 3157–3179. [[CrossRef](#)]
26. Yao, W.; Lin, H.; Derome, J. Submonthly Forecasting of Winter Surface Air Temperature in North America Based on Organized Tropical Convection. *Atmos. Ocean* **2011**, *49*, 51–60. [[CrossRef](#)]
27. Grise, K.M.; Son, S.-W.; Gyakum, J.R. Intraseasonal and Interannual Variability in North American Storm Tracks and Its Relationship to Equatorial Pacific Variability. *Mon. Weather Rev.* **2013**, *141*, 3610–3625. [[CrossRef](#)]
28. Goss, M.; Feldstein, S.B. The impact of the initial flow on the extratropical response to Madden–Julian oscillation convective heating. *Mon. Weather Rev.* **2015**, *143*, 1104–1121. [[CrossRef](#)]
29. Lin, H.; Brunet, G.; Derome, J. The nonlinear transient atmospheric response to tropical forcing. *J. Clim.* **2007**, *20*, 5642–5665. [[CrossRef](#)]
30. Jin, F.; Hoskins, B.J. The direct response to tropical heating in a baroclinic atmosphere. *J. Atmos. Sci.* **1995**, *52*, 307–319. [[CrossRef](#)]
31. Moon, J.Y.; Wang, B.; Ha, K.J. MJO Modulation on 2009/10 winter snowstorms in the United States. *J. Clim.* **2012**, *25*, 978–991. [[CrossRef](#)]
32. Roundy, P.E.; MacRitchie, K.; Asuma, J.; Melino, T. Modulation of the global atmospheric circulation by combined activity in the Madden–Julian Oscillation and the El Niño–Southern Oscillation during Boreal winter. *J. Clim.* **2010**, *23*, 4045–4059. [[CrossRef](#)]
33. Hendon, H.H.; Wheeler, M.C.; Zhang, C. Seasonal Dependence of the MJO–ENSO Relationship. *J. Clim.* **2007**, *20*, 531–543. [[CrossRef](#)]
34. Hoell, A.; Barlow, M.; Wheeler, M.C.; Funk, C. Disruptions of El Niño–Southern Oscillation Teleconnections by the Madden–Julian Oscillation. *Geophys. Res. Lett.* **2014**, *41*, 998–1004. [[CrossRef](#)]
35. Bell, G.D.; Janowiak, J.E. Atmospheric Circulation Associated with the Midwest Floods of 1993. *Bull. Am. Meteorol. Soc.* **1995**, *76*, 681–695. [[CrossRef](#)]

